SOME MONITORING PROCEDURES RELATED TO ASYMMETRY PARAMETER OF AZZALINI'S SKEW-NORMAL MODEL

Authors: CHENGLONG LI
– School of Management, Xi'an Jiaotong University, Xi'an, China
  Department of Systems Engineering and Engineering Management,
  City University of Hong Kong, Hong Kong, China
  lchenglon2-c@my.cityu.edu.hk

AMITAVA MUKHERJEE
– Production, Operations and Decision Sciences Area,
  XLRI-Xavier School of Management, Jamshedpur, India
  amitmukh2@yahoo.co.in

QIN SU
– School of Management, Xi'an Jiaotong University, Xi'an, China
  qinsu@mail.xjtu.edu.cn

MIN XIE
– Department of Systems Engineering and Engineering Management,
  City University of Hong Kong, Hong Kong, China
  minxie@cityu.edu.hk

Abstract:

• In the real world, we often observe that the underlying distribution of some Gaussian processes tends to become skewed, when some undesirable assignable cause takes place in the process. Such phenomena are common in the field of manufacturing and in chemical industries, among others, where a process deviates from a normal model and becomes a skew-normal. The Azzalini's skew-normal (hereafter ASN) distribution is a well-known model for such processes. In other words, we assume that the in-control (hereafter IC) distribution of the process under consideration is normal, that is a special case of the ASN model with asymmetry parameter zero, whereas the out-of-control (hereafter OOC) process distribution is ASN with any non-zero asymmetry parameter. In the ASN model, a change in asymmetry parameter also induces shifts in both the mean and variance, even if, both the location and scale parameters remain invariant. Traditionally, researchers consider a shift either in the mean or in variance or in both the parameters of the normal distribution. Some inference and monitoring issues related to deviation from symmetry are essential problems that are largely overlooked in literature. To this end, we propose various test statistics and design for sequential monitoring schemes for the asymmetry parameter of the ASN model. We examine and compare the performance of various procedures based on an extensive Monte-Carlo experiment. We provide an illustration based on an interesting manufacturing case study. We also offer some concluding remarks and future research problems.

Key-Words:

- *disruption of symmetry; distance skewness; maximum likelihood estimator; Monte-Carlo simulations; skew-normal distribution; statistical process monitoring.*

AMS Subject Classification:

- 62F03, 62P30, 65C05, 90B99.

1.   INTRODUCTION
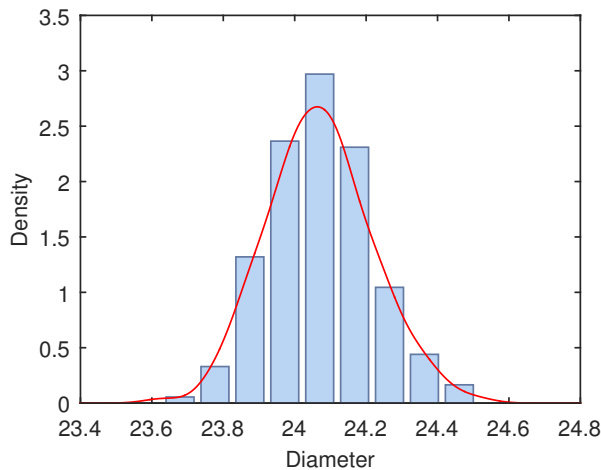
In many of the practical applications, a univariate process characteristic, such as the warp length of semiconductor wafers, or the diameter of piston rings among others, is assumed to follow a normal distribution. A normal distribution can be completely specified by its mean (μ) and variance (σ^2), the two parameters of the distribution. In standard quality control literature, a number of control charts are developed and studied for detecting a shift in mean (also called location parameter), among them by Tsiamyrtzis and Hawkins [37], Ryu *et al.* [31], Khoo *et al.* [18], Peng *et al.* [26], and many others. Similarly, there are host of research articles for detection of a shift in variance or the scale parameter (σ), such as, Castagliola [6], Shu *et al.* [33], Zhang [40], Guo and Wang [14], among others. In the recent years, several researchers have also addressed the problem of jointly monitoring both the location and scale parameters of a normally distributed process. We recommend reading Hawkins and Deng [15], Wu *et al.* [39], Sheu *et al.* [32], McCracken *et al.* [24], Reynolds *et al.* [29], Knoth [19] and Li *et al.* [20], among others, for more details.

Despite a great progress of parametric testing of hypothesis and process monitoring, we, traditionally, assume that the parent population distribution of the process characteristic remains normal and only change takes place in the parameters of the distribution. Generally, we assume that the shift may occur either in its mean or variance or in both. Nevertheless, this assumption is more often very stringent. There are other ways in which a normally distributed process may change. Ross and Adams [30] stated that, in many real-life applications, it could be desirable to monitor for a change in the shape of the process distribution. Similar arguments can also be found in Zou and Tsung [41] and Li *et al.* [22]. Normal distribution is well known as a symmetric bell-shaped distribution and in consequence when a shift occurs in normal distribution, it may tend to become skewed or asymmetric.

This phenomenon, in fact, is quite common in practice, especially in physical, chemical or geological research field. Vincent and Walsh [38] indicated that the experimental intensity distributions in convergent beam electron diffraction patterns always exhibit deviations from ideal symmetry, attributable to the causes, such as, strain, inclined surfaces, incomplete unit cells and imperfections in the electron optics. Rahman and Hossain [27] showed another very relevant example, about the groundwater arsenic contamination in Bangladesh. They noted that the transmission of contaminants can affect the symmetric nature of the distribution of arsenic concentration, being positively skewed. Interested readers may also see Mukherjee *et al.* [25] for more details. In the context of statistical process monitoring, Figueiredo and Gomes [9] studied a real industrial example related to the diameters of cork stoppers produced by a manufacturing unit and

noted that the data nicely follows an ASN distribution. After a close examination, we find that the distribution of the diameters of the cork was actually normal in the initial phase and slowly it tends to become skew-normal. Figure 1 shows the histogram and density estimate of the first 200 diameter observations from the production data set of Figueiredo and Gomes [9], which has altogether 1000 observations. The p-value of the Shapiro-Wilk normality test for the first 200 observations is 0.9296 which strongly supports the normality assumption in the initial stage of production. Naturally, we can imagine that the process is shifted from a normal distribution to an ASN distribution in the later stage of production. We provide a detailed illustration with the cork stoppers' data later in Section 5.

Figure 1: Histogram and density estimate of the first 200 diameter observations.

In the nice work, Ferreira and Steel [8] proposed a constructive representation of skewed distributions and provided three common methods of generating univariate skewed distributions, namely, hidden truncation, inverse scale factors, and order statistics. Among them, the skew-normal distribution of Azzalini [2] is probably the most common and most intensively studied one from diverse areas of application and is developed with the idea—hidden truncation. The statistical properties of ASN distribution and its variations have been discussed by several authors and many similarities with the ordinary normal distribution are observed, see for example, Azzalini [2, 3], Henze [16], Genton *et al.* [12], Arellano-Valle *et al.* [1], Chen *et al.* [7], Azzalini [4], Gómez *et al.* [13], Mameli and Musio [23], Su and Gupta [35]. Various researches established that the ASN family of distributions have rather important roles to play in the production practice, such as, modeling real datasets or simulating skewed data with different degrees of asymmetry and tail-weight. Interested readers may see, among others, Chen *et al.* [7], Bartoletti

and Loperfido [5], Fruhwirth-Schnatter and Pyne [11], Razzaghi [28], Figueiredo and Gomes [10]. Nevertheless, there are merely few research articles that have addressed the process monitoring issues with ASN distributions. The problems related to process monitoring are considered in Tsai [36], Figueiredo and Gomes [9], Su *et al.* [34], Li *et al.* [21]. The major theme of these researches is, however, the construction of control charts for skewed data, that includes detection of shifts in location and/or scale. Needless to say that the problem of monitoring and detecting departures from normality, i.e., from the normal to skew-normal, has not been considered yet. Such a distributional change might not be readily spotted by some traditional control charting schemes, such as the $\overline{X}$ chart and S chart, because they are not designed for that purpose. Our current work aims at addressing this long-standing problem in the context of process monitoring and attempts to bridge the existing research gap.

The rest of this paper is organized as follows: Section 2 provides some information about ASN distribution and also introduces several competitive test statistics for the purpose of detecting the disruption of symmetry of a normally distributed process characteristic. The respective sequential monitoring procedures, as well as the determination of their design parameters are presented in Section 3. An extensive performance comparison and analysis is included in Section 4. Section 5 illustrates the real example based on the corks' diameter data from Figueiredo and Gomes [9]. Finally, we offer some concluding remarks and problems for future research in Section 6.

2. SOME STATISTICAL TESTS FOR ASYMMETRY PARAMETER

Let X be the continuous random variable (r.v.) denoting the process characteristic subject to testing or monitoring. The r.v. X is said to follow ASN distribution if its probability density function (pdf) is of the form:
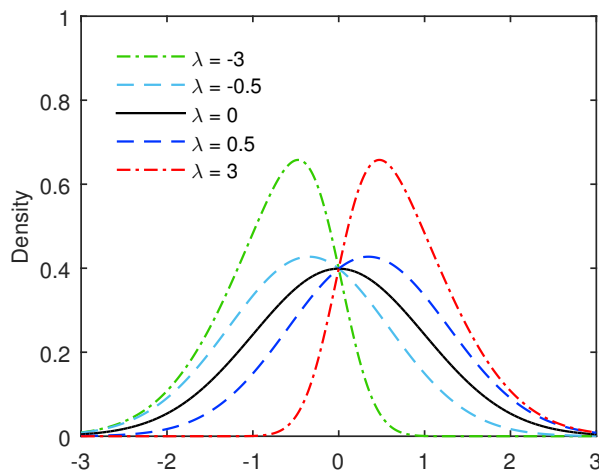
$$f(x; \xi, \omega, \lambda) = \frac{2}{\omega} \phi\left(\frac{x-\xi}{\omega}\right) \Phi\left(\lambda \frac{x-\xi}{\omega}\right), \quad -\infty < x < \infty,$$

$$-\infty < \xi < \infty, \quad -\infty < \lambda < \infty, \quad \omega > 0,$$

where ξ is the location parameter, ω is the scale parameter, and λ is the asymmetry parameter, also called shape parameter; $\phi(\cdot)$ and $\Phi(\cdot)$ are the pdf and cumulative distribution function (cdf) of the standard normal distribution, respectively. In a standard notation, we express it as $X \sim ASN(\xi, \omega, \lambda)$.

The ASN distribution is positively skewed if $\lambda > 0$, and is negatively skewed if $\lambda < 0$. The critical parameter λ controls the skewness of the distribution (see Figure 2). Note that, when $\lambda = 0$, the ASN distribution boils down to a normal

distribution with mean $\mu = \xi$ and variance $\sigma^2 = \omega^2$, which implies that normal distribution is a special case of the ASN family of distributions. Accordingly, the ordinary normal distribution can also be denoted as $X \sim ASN(\xi, \omega, 0)$, instead of $X \sim N(\mu, \sigma^2)$.

Figure 2:   The pdf of Azzalini's SN distribution.

The variation of asymmetry parameter λ in ASN distribution automatically changes its mean and variance. If the distribution shifts from $ASN(\xi_0, \omega_0, 0)$ to $ASN(\xi_0, \omega_0, \lambda)$, it is easy to see that the changed mean $\mu_1 = \mu_0 + \lambda\sigma_0\sqrt{\frac{2}{\pi(1+\lambda^2)}}$ and variance $\sigma_1^2 = \left(1 - \frac{2\lambda^2}{\pi(1+\lambda^2)}\right)\sigma_0^2$ where we have $\mu_0 = \xi_0$ and $\sigma_0 = \omega_0$. In this context, if we apply a simultaneous testing or monitoring scheme, designed for the mean and variance of a normal model, we often get illusive results as the shifted model no longer follows normal distribution. A more practical problem is to test or monitor the asymmetry parameter of ASN distribution or all the parameters of the ASN distribution. In this paper, we only consider the inference and monitoring problems related to the asymmetry parameter λ of the ASN distribution and assume both the location and scale parameters remain invariant and known. In other words, we consider the problem of sequential monitoring of the ideal condition of $\lambda = 0$. Further research on simultaneous monitoring of all the parameters may be taken separately as a highly warranted research problem. In the present context, we assume that ξ_0 and ω_0, the process location and scale or the mean and variance of the normally distributed IC process are known. This assumption is realistic as practitioners commonly have a fair idea about the process parameters either based on certain target set-up of the companies or based on the prior knowledge about the distribution of process characteristics.

We first consider the tests based on the likelihood ratio criterion, and the moment estimator for the asymmetry parameter λ. Noting that ad-hoc inference

is gaining more and more popularity, we also introduce several ad-hoc statistics for tracking skewness which is related to the value of λ. In the subsequent subsections, we introduce these statistics and the tests based on them.

2.1. Likelihood ratio test

Let $\boldsymbol{x_n} = (x_1, x_2, ..., x_n)$ be the sample of size n drawn from the r.v. X with $X \sim ASN(\xi, \omega, \lambda)$. Given $\boldsymbol{x_n}$, the log-likelihood function for λ is given by

$$l(\lambda | \boldsymbol{x_n}, \mu_0, \sigma_0) = n\ln 2 - n\ln\sigma_0 + \sum_{i=1}^{n} \ln\phi\left(\frac{x_i - \mu_0}{\sigma_0}\right) + \sum_{i=1}^{n} \ln\Phi\left(\lambda\frac{x_i - \mu_0}{\sigma_0}\right).$$

Writing $z_i = \frac{x_i - \mu_0}{\sigma_0}$, we can obtain the maximum likelihood (ML) estimator of λ, say $\hat{\lambda}_{MLE}$, as the solution of

$$\frac{dl}{d\lambda} = \sum_{i=1}^{n} \frac{z_i \phi(\lambda z_i)}{\Phi(\lambda z_i)} = 0.$$

In the language of theory of testing of statistical hypothesis, if we consider the problem of testing H_0: $X \sim ASN(\xi_0, \omega_0, \lambda_0 = 0)$, that is, $X \sim N(\mu_0, \sigma_0^2)$ against H_1: $X \sim ASN(\xi_0, \omega_0, \lambda_1)$, a likelihood ratio criterion can be given by:

$$\Lambda(\boldsymbol{x_n} | \mu_0, \sigma_0) = \frac{1}{2^n \prod_{i=1}^{n} \Phi\left(\hat{\lambda}_{MLE} z_i\right)}.$$

We reject H_0 at a given level of significance if $\Lambda(\boldsymbol{x_n} | \mu_0, \sigma_0) < c_{LR}$, where c_{LR} is a pre-determined constant that satisfies the level criterion. Note that, $\Lambda(\boldsymbol{x_n} | \mu_0, \sigma_0) < c_{LR}$, indeed, is equivalent to $T = -2\ln\Lambda(\boldsymbol{x_n} | \mu_0, \sigma_0) = 2n\ln 2 + 2\sum_{i=1}^{n} \ln\Phi\left(\hat{\lambda}_{MLE} z_i\right) > -2\ln c_{LR}$. Thus, writing $c_{LR}^* = -2\ln c_{LR}$, the critical region of the test may be given by $T > c_{LR}^*$.

Using the nice analogy between theory of testing of hypothesis and statistical process control, we can easily develop a sequential monitoring procedure based on T. It is known that, under the null hypothesis, T follows a chi-squared distribution with 1 degree of freedom if n is large. However, we found that this approximation is useful if the test sample size n is at least 100. For small n, the approximation is not at all satisfactory. In the context of statistical process monitoring, test sample sizes are usually very small, say $n = 5$ or 10 or 25. A sample size of $n > 100$ is very rare in practice and in quality control literature. Therefore, we omit the asymptotic theory related to T in subsequent analysis and discussion. Instead, we choose to work with the simulated distribution of T traced via Monte-Carlo.

2.2. Test based on the moment estimators

2.2.1. Inadmissibility of test based on method of moments estimator

Unlike the ML estimation, the method of moments (MM) to estimate λ may be obtained more explicitly using the sample skewness, say $\hat{\gamma}$, by inverting the skewness equation given as:

$$|\delta| = \sqrt{\frac{\pi}{2} \frac{|\hat{\gamma}|^{\frac{2}{3}}}{|\hat{\gamma}|^{\frac{2}{3}} + \left(\frac{4-\pi}{2}\right)^{\frac{2}{3}}}}, \qquad \delta = \frac{\lambda}{\sqrt{1+\lambda^2}},$$

where the sign of δ is the same as the sign of $\hat{\gamma}$ and thus, we can derive the MM estimator of λ, say $\hat{\lambda}_{MME} = \frac{\delta}{\sqrt{1-\delta^2}}$. Note that here theoretically the maximum skewness is obtained by setting $\delta = 1$, which gives $\hat{\gamma}$ approximately equal to 0.99527. Nevertheless, in practice, it may happen that the observed sample skewness is larger. In such situations, $\hat{\lambda}_{MME}$ cannot be obtained from the above equation. Admittedly, we may consider a trade-off by letting $|\hat{\gamma}| = 0.99527$ when the obtained $|\hat{\gamma}|$ is coincidentally greater than 0.99527.

Interestingly, we have found that the MM estimation, in the present context, is rather inefficient especially for small-to-moderate sample size. We observe with $n = 5$, when the process is IC, the probability that the sample skewness exceeds 0.99527 is about 12.2%. That is, we cannot construct a nontrivial exact test at 5% level in this context. If $n = 15$, 25 and 50 the probability of the same event becomes 5.9%, 2.7%, and 0.5% respectively. In the process monitoring context, with $n = 50$, we may construct a sequential inspection scheme that will allow us to achieve a maximum IC average run length: $IC\text{-}ARL = \frac{1}{0.005} = 200$. This is certainly undesirable and thus, we drop this statistic from further discussion.

2.2.2. Estimator based on L-moments

L-moments are a sequence of statistics used to summarize the shape of a probability distribution. They are linear combinations of the order statistics analogous to conventional moments. Let $x_1, x_2, ..., x_n$ be the sample and $x_{(1)} \leq x_{(2)} \leq \cdots \leq x_{(n)}$ be the ordered sample, and direct estimators for the first three L-moments in a finite sample of n observations are defined to be (see Hosking [17])

$$l_1 = n^{-1}\sum_i x_i,$$

$$l_2 = \frac{1}{2}\binom{n}{2}^{-1}\sum_i\sum_j\left(x_{(i)} - x_{(j)}\right), \qquad \text{for} \quad i > j\,,$$

$$l_3 = \frac{1}{3}\binom{n}{3}^{-1}\sum_i\sum_j\sum_k\left(x_{(i)} - 2x_{(j)} + x_{(k)}\right), \qquad \text{for} \quad i > j > k\,.$$

The L-skewness is estimated by $L = l_3/l_2$. The L-skewness is a coefficient that measures the degree of asymmetry and may take on positive or negative values. It is known that $0 \le |L| < 1$, where $L = 0$ indicates a possible symmetry. Therefore, we can consider a test based on $|L|$ and reject H_0 at a given level of significance if $|L| > c_{LS}$, where c_{LS} is a pre-determined constant satisfies the level criterion.

2.3. Ad-hoc approaches

2.3.1. Test based on the sample skewness statistic

Instead of the MM estimation, the sample skewness, $\hat{\gamma}$, may be directly adopted to track the skewness of the process distribution and judge whether there is a shift from $\lambda = 0$. The form of sample skewness is given by

$$\hat{\gamma} = \frac{\frac{1}{n}\sum_{i=1}^{n}\left(x_i - \overline{x}\right)^3}{\left[\frac{1}{n}\sum_{i=1}^{n}\left(x_i - \overline{x}\right)^2\right]^{3/2}}\,,$$

where $\overline{x}$ denotes the mean of the sample of size n. In general, we expect that under symmetry, $\hat{\gamma}$ should be closer to 0. Under positive or negative skewness, we generally expect that $\hat{\gamma}$ is greater than or less than 0 respectively. If we are interested in detecting a general two-sided shift (both left or right skewness) from symmetry, we prefer a test based on $|\hat{\gamma}|$ and reject H_0 at a given level of significance if $|\hat{\gamma}| > c_{SS}$, where c_{SS} is a pre-determined constant satisfies the level criterion.

2.3.2. Test based on the distance skewness statistic

There is a simple consistent statistical test of diagonal symmetry based on the sample distance skewness:

$$D = 1 - \frac{\sum_{i,j}|z_i - z_j|}{\sum_{i,j}|z_i + z_j|}\,,$$

where the z's are the standardized observations in a sample. The sample distance skewness can be used as a way to decide whether there is a shift from $\lambda = 0$. Its value is always between 0 and 1, and in general, it is expected that under symmetry, $D = 0$ and under positive or negative skewness, D is expected to be greater than 0. Thus, the statistic D can be considered for two-sided test of H_0: $\lambda = 0$ versus H_1: $\lambda \neq 0$. We reject H_0 at a given level of significance if $D > c_{DS}$, where c_{DS} is a pre-determined constant satisfies the level criterion.

2.3.3. Test based on the median skewness statistic

The Pearson's median skewness, or second skewness coefficient, is defined by

$$M = 3\frac{(\overline{x} - \tilde{x})}{s},$$

where $\tilde{x}$ is the sample median and s is the sample standard deviation of size n. It is a simple multiple of the nonparametric skew. In general, it is expected that under symmetry, $\overline{x} = \tilde{x}$ and consequently $M = 0$. Under positive or negative skewness, in general, we expect M greater than or less than 0 respectively. Therefore, we may reject H_0 at a given level of significance if $|M| > c_{MS}$, where c_{MS} is a pre-determined constant satisfies the level criterion.

2.3.4. Quantile-based approach

Writing Q_i, $i = 1, 2, 3$ as the ith quartile of the distribution, the Bowley's measure of skewness is given by

$$B = \frac{Q_3 - 2Q_2 + Q_1}{Q_3 - Q_1}.$$

It is expected that for a normal distribution $B = 0$ and for an ASN distribution $B > 0$ or $B < 0$ according as $\lambda > 0$ or $\lambda < 0$. Therefore, for simplicity one can use B to verify whether the symmetry condition of the normal distribution remains valid or an asymmetric pattern creeps in. For two-sided monitoring, we may use $|B|$ as the monitoring statistic. We reject H_0 at a given level of significance if $|B| > c_{BS}$, where c_{BS} is a pre-determined constant satisfies the level criterion.

3. DESIGN AND IMPLEMENTATION OF SEQUENTIAL MONITORING OF ASYMMETRY PARAMETER

From production and manufacturing to various other sectors, often sequential monitoring and control of process parameter is of primary interest. In this section, we present six monitoring procedures based on the test statistics, respectively, introduced in Section 2. These statistics are

(a) the likelihood ratio statistic T,

(b) the L-skewness statistic $|L|$,

(c) the sample skewness statistic $|\hat{\gamma}|$,

(d) the sample distance skewness statistic D,

(e) the median skewness statistic $|M|$, and

(f) the Bowley's statistic $|B|$.

Thus, we consider the following six schemes (A-F) for sequential monitoring of asymmetry parameter.

A: The NSN-LR chart based on likelihood ratio statistic as in Section 2.1;

B: The NSN-LS chart based on L-skewness as in Section 2.2.2;

C: The NSN-SS chart based on sample skewness as in Section 2.3.1;

D: The NSN-DS chart based on sample distance skewness as in Section 2.3.2;

E: The NSN-MS chart based on median skewness as in Section 2.3.3;

F: The NSN-BS chart based on Bowley's measure of skewness as in Section 2.3.4.

The abbreviation NSN is used to highlight the purpose of detecting a shift from Normal(N) to Skew-Normal (SN). We first consider the sequential monitoring procedure based on the NSN-LR chart. The method of constructing a NSN-LR chart involves the following steps:

Step-1: Collect $\boldsymbol{x_{jn}} = (x_{j1}, x_{j2}, ..., x_{jn})$, the jth test sample from the process for $j = 1, 2, ...$ Clearly, n is the fixed sample size for the jth test sample or the so called rational subgroup.

Step-2: Compute the plotting statistic: $T_j = 2n\ln 2 + 2\sum_{i=1}^{n} \ln\Phi\left(\hat{\lambda}_{MLE} z_{ji}\right)$.

Step-3: Plot T_j against an upper control limit (UCL) H_{LR}. The lower control limit (LCL) is by default 0, noting that $T_j \geq 0$ by definition as $\Lambda\left(\boldsymbol{x_{jn}}|\mu_0, \sigma_0\right)$ takes a value between 0 and 1.

Step-4: If T_j exceeds H_{LR}, the process is declared OOC at the jth test sample. If not, the process is considered to be IC, and testing continues to the next sample.

The sequential monitoring procedures based on other statistics are very similar except for the steps related to computing the plotting statistics and using corresponding control limits. Therefore, we omit the details for brevity.

It is easy to note that we are basically considering standard Phase-II Shewhart-type charts with standards known (Case-K). Consequently, the run-length distribution will be exactly geometric. Consider any statistic U and corresponding UCL as H_U. The expected IC run length can be expressed in terms of probabilities: $p_U(H_U) = P[U_j > H_U|\text{IC}]$. Let $F_U(\cdot)$ be the cdf of the plotting statistic under IC set-up. Then, we can also write $p_U(H_U) = 1 - F_U(H_U)$. In the present context, we identify U with T, $|L|$, $|\hat{\gamma}|$, D, $|M|$ and $|B|$, respectively, for the schemes A to F discussed above. Further, we identify H_U with H_{LR}, H_{LS}, H_{SS}, H_{DS}, H_{MS} and H_{BS}, respectively, for these six schemes.

Table 1:   The UCL values for the NSN charts.

n	The NSN-LR chart: H_{LR}			The NSN-LS chart: H_{LS}		
	IC-ARL $=250$	IC-ARL $=370$	IC-ARL $=500$	IC-ARL $=250$	IC-ARL $=370$	IC-ARL $=500$
5	6.9315*	6.9315*	6.9315*	0.7980	0.8208	0.8383
10	10.1944	11.2063	12.2779	0.4754	0.4942	0.5086
15	9.0789	9.9548	10.6227	0.3615	0.3754	0.3854
20	8.8727	9.6034	10.2425	0.3090	0.3215	0.3292
25	8.6560	9.4490	9.9779	0.2689	0.2795	0.2896
30	8.5876	9.3119	9.8591	0.2442	0.2534	0.2610
50	8.4382	9.2416	9.7183	0.1831	0.1906	0.1957

n	The NSN-SS chart: H_{SS}			The NSN-DS chart: H_{DS}		
	IC-ARL $=250$	IC-ARL $=370$	IC-ARL $=500$	IC-ARL $=250$	IC-ARL $=370$	IC-ARL $=500$
5	1.4429	1.4557	1.4631	0.8185	0.8364	0.8496
10	1.7707	1.8493	1.9050	0.5760	0.6018	0.6197
15	1.6327	1.7181	1.7797	0.4355	0.4609	0.4793
20	1.5028	1.5848	1.6484	0.3501	0.3707	0.3854
25	1.3948	1.4670	1.5286	0.2925	0.3122	0.3259
30	1.2815	1.3587	1.4126	0.2530	0.2691	0.2815
50	1.0233	1.0797	1.1331	0.1638	0.1762	0.1857

n	The NSN-MS chart: H_{MS}			The NSN-BS chart: H_{BS}		
	IC-ARL $=250$	IC-ARL $=370$	IC-ARL $=500$	IC-ARL $=250$	IC-ARL $=370$	IC-ARL $=500$
5	1.9909	2.0165	2.0360	0.9459	0.9555	0.9623
10	1.5366	1.5842	1.6173	0.8638	0.8797	0.8929
15	1.5111	1.5614	1.6003	0.7998	0.8221	0.8350
20	1.2690	1.3147	1.3444	0.7011	0.7206	0.7367
25	1.2227	1.2652	1.3003	0.6722	0.6916	0.7061
30	1.0807	1.1178	1.1545	0.6242	0.6452	0.6607
50	0.8815	0.9154	0.9506	0.5149	0.5339	0.5464

Note: * indicates invalid UCL values.

In general, the charts are designed such that the appropriate UCL is found for a desired nominal $IC\text{-}ARL$ or called ARL_0. Now equating expected run length with the target $IC\text{-}ARL$, we have $IC\text{-}ARL = \frac{1}{p_U(H_U)}$ from which we can find expression for H_U in terms of the target $IC\text{-}ARL$. To this end, we use a Monte-Carlo simulation with adequate replicates (100,000 times) and acquire the appropriate quantile based on the empirical distribution function for realizing the target $IC\text{-}ARL$. Throughout the paper, we adopt this simulation technique, and in Table 1, we offer some UCL values for these aforementioned NSN charts for various test sample size n and for various nominal $IC\text{-}ARL$ values.

From the UCL values of Table 1, we observe that H_{LR} and H_{SS} increase initially when n is small and then decrease gradually when n is relatively larger, while for the other charts UCL values decrease monotonically within the purview of range of n considered here, that is, $n \leq 50$. It is worth mentioning that it is difficult to obtain UCL values for the NSN-LR chart for some common $IC\text{-}ARL$ context, when test sample size is small, say, $n < 10$. This is not surprising as Figueiredo and Gomes [9] noted that small n may often produces boundary estimates. The log-likelihood function will be an increasing (decreasing) function of λ if all observations are positive (negative). Nevertheless, overall performance of the NSN-LR chart is very encouraging in most cases, as long as the test sample size is not too small.

4. PERFORMANCE ANALYSIS FOR QUICKEST DETECTION

4.1. The performance comparisons between NSN charts

In the present paper, clearly the IC value of λ is $\lambda_0 = 0$. To compare these NSN charts thoroughly and for performance analysis, we choose the shifted (OOC) value of λ as $\lambda_1 = 0.3$, 0.5, 1, 2, 3, 5, 10, for drawing Phase-II samples. Without loss of generality, for both the IC or OOC situations, we consider $\mu_1 = \mu_0 = 0$ and $\sigma_1 = \sigma_0 = 1$. For specified n and $IC\text{-}ARL$ ($= 370$), we compute the ARL and the standard deviation of the run length ($SDRL$). Our findings for $n = 5$, 10, 15, 25 are summarized in Table 2. For some other values of $IC\text{-}ARL$ (say, 250 and 500), the results are comparable and consistent, and therefore, we omit the details for brevity.

First we notice that, for specified test sample size n, the ARL and the $SDRL$ of all the NSN charts decrease steeply with the increasing shift in λ. Further, when n increases, in general, we see that for any NSN scheme, baring some sampling fluctuations, both the ARL and $SDRL$ tend to decrease. Precisely, the larger the value of n is, the quicker the detection of a specified magnitude of shift will be.

For the NSN-BS chart, however, the rate of change of *OOC-ARL* with n is very slow.

Table 2:   The OOC performance comparisons between NSN charts
for various λ_1 and n when *IC-ARL* = 370.

λ_1	$n = 5$					
	NSN-LR chart	NSN-LS chart	NSN-SS chart	NSN-DS chart	NSN-MS chart	NSN-BS chart
0.3		365.94 (367.66)	361.33 (362.72)	**230.85 (229.96)**	360.92 (359.35)	354.16 (354.21)
0.5		365.94 (363.62)	360.13 (361.32)	**145.69 (145.00)**	360.37 (359.34)	352.48 (351.78)
1		358.65 (357.29)	353.72 (353.22)	**60.77 (60.21)**	361.97 (362.68)	351.79 (352.46)
2	Not Useful	314.71 (314.08)	310.02 (310.61)	**30.19 (29.60)**	352.62 (352.00)	337.77 (338.82)
3		268.01 (267.64)	263.68 (263.41)	**24.70 (24.12)**	329.34 (328.60)	311.48 (310.98)
5		214.00 (213.31)	210.57 (209.94)	**22.45 (21.87)**	288.18 (287.75)	271.05 (270.74)
10		171.76 (170.93)	170.43 (169.73)	**21.97 (21.41)**	244.67 (243.94)	228.48 (227.81)

λ_1	$n = 10$					
	NSN-LR chart	NSN-LS chart	NSN-SS chart	NSN-DS chart	NSN-MS chart	NSN-BS chart
0.3	129.81 (128.97)	360.69 (360.97)	362.55 (362.36)	**123.92 (122.95)**	350.36 (351.69)	375.60 (375.65)
0.5	55.69 (54.73)	357.54 (357.25)	360.44 (359.63)	**51.78 (51.16)**	350.22 (349.81)	374.47 (371.86)
1	13.06 (12.53)	325.34 (325.80)	322.95 (320.52)	**12.04 (11.53)**	350.59 (350.57)	373.06 (372.07)
2	**3.78 (3.23)**	187.36 (186.80)	178.54 (177.59)	3.84 (3.31)	302.18 (302.43)	353.01 (354.16)
3	**2.31 (1.74)**	111.74 (111.11)	111.15 (109.89)	2.61 (2.05)	229.49 (228.47)	319.94 (320.17)
5	**1.55 (0.93)**	64.90 (64.73)	73.35 (72.47)	2.01 (1.43)	149.87 (149.05)	279.57 (280.26)
10	**1.18 (0.46)**	44.29 (43.99)	57.45 (56.79)	1.75 (1.15)	103.43 (103.09)	253.59 (254.70)

λ_1	$n = 15$					
	NSN-LR chart	NSN-LS chart	NSN-SS chart	NSN-DS chart	NSN-MS chart	NSN-BS chart
0.3	**73.57 (73.20)**	329.54 (328.94)	338.05 (336.81)	74.68 (74.47)	354.19 (353.90)	380.89 (379.71)
0.5	**24.61 (24.10)**	326.13 (326.26)	334.20 (335.13)	24.98 (24.46)	353.86 (353.78)	378.44 (376.32)
1	**4.56 (4.02)**	279.58 (279.16)	269.27 (267.96)	4.80 (4.25)	353.81 (352.84)	375.84 (377.41)
2	**1.46 (0.82)**	115.69 (115.01)	112.15 (112.21)	1.62 (1.00)	282.86 (282.64)	345.41 (343.83)
3	**1.11 (0.35)**	56.16 (55.43)	62.81 (62.63)	1.23 (0.53)	190.95 (190.35)	294.50 (293.73)
5	**1.01 (0.11)**	28.17 (27.46)	39.39 (39.11)	1.07 (0.28)	108.10 (107.82)	235.77 (236.28)
10	**1.00 (0.01)**	17.96 (17.40)	30.27 (29.69)	1.02 (0.16)	69.06 (68.37)	204.56 (203.73)

λ_1	$n = 25$					
	NSN-LR chart	NSN-LS chart	NSN-SS chart	NSN-DS chart	NSN-MS chart	NSN-BS chart
0.3	**35.52 (34.95)**	367.13 (366.06)	370.12 (371.24)	36.60 (36.09)	345.62 (346.94)	357.06 (358.49)
0.5	**9.49 (9.00)**	361.87 (361.88)	361.69 (362.16)	9.99 (9.50)	346.00 (346.17)	355.45 (355.78)
1	**1.80 (1.21)**	276.97 (276.77)	250.80 (250.88)	1.93 (1.34)	333.34 (332.28)	350.34 (351.09)
2	**1.02 (0.16)**	70.21 (69.51)	69.69 (69.30)	1.05 (0.22)	198.51 (197.95)	294.49 (293.77)
3	**1.00 (0.03)**	26.42 (25.85)	33.83 (33.27)	**1.00 (0.06)**	99.94 (99.03)	218.99 (217.80)
5	**1.00 (0.00)**	11.43 (10.87)	19.29 (18.75)	**1.00 (0.01)**	45.51 (45.03)	153.77 (153.12)
10	**1.00 (0.00)**	6.90 (6.40)	14.31 (13.86)	**1.00 (0.00)**	28.00 (27.58)	130.94 (130.07)

For a given n and λ_1, we compare the schemes in terms of *OOC-ARL*, and consider a scheme the best, if it offers the lowest *OOC-ARL*. The cells correspond to the best performing chart are shown in bold typeface in the tables. We further see from Table 2 that the NSN-LR chart and the NSN-DS chart are uniformly superior to the other four NSN charts. The NSN-DS chart is particularly well suited for the cases where n is small (e.g., $n = 5$), where the NSN-LR chart is inadmissible, as mentioned earlier. The two charts, namely, NSN-LR chart and

NSN-DS chart, perform rather similarly with a moderate-to-large test sample size (say $n \geq 10$), though the NSN-LR chart displays a slight advantage over the NSN-DS chart. Besides, both these charts have a rather low *OOC-ARL* value when n is large, even if, the shift in λ is relatively small. The rest four NSN charts perform poorly in almost all cases. The NSN-SS chart, the NSN-MS chart and the NSN-LS chart are very inefficient when n is small and shift size is also small, however, under large n, and for large shift size, the performance of these charts improves significantly. Nevertheless, even with $n = 50$ and $\lambda_1 = 10$, these schemes are inferior compared with the NSN-LR chart or the NSN-DS chart. Unfortunately, the NSN-BS chart is the worst and is practically useless.

Based on the results displayed in Table 2, we highly recommend the NSN-LR chart and the NSN-DS chart for detecting the shift from normal to skew-normal, especially the latter. The NSN-DS chart has a broader scope of application in practice than the NSN-LR chart as it is effective even if the test sample size is small where the NSN-LR chart is inadmissible. Further, we almost always see that the NSN-DS chart performs very close to the NSN-LR chart when the NSN-LR chart is the best in terms of *OOC-ARL* values. Therefore, the NSN-DS chart is very competitive, and moreover, it may be more preferable to the users taking into account the simplicity of implementation and its inherent ability to detect a deviation from symmetry. Nevertheless, from the performance perspective, we recommend both charts and the users can have a choice to adopt the NSN-LR chart or the NSN-DS chart according to their practical requirement. The rest four NSN charts based on common measures of skewness are much more inefficient and we suggest not to use them.

4.2. The comparisons to traditional charts for mean and/or variance

We have noted earlier that when the underlying process distribution deviates from normality and becomes skew-normal, as a result of a shift in the asymmetry parameter λ from 0, the process mean and variance also change. The mean and variance of the shifted process are given respectively by $\mu_1 = \mu_0 + \lambda_1 \sigma_0 \sqrt{\frac{2}{\pi(1+\lambda_1^2)}}$ and $\sigma_1^2 = \left(1 - \frac{2\lambda_1^2}{\pi(1+\lambda_1^2)}\right)\sigma_0^2$. Therefore, one may argue that it might be still meaningful to employ traditional process control schemes to monitor process mean, or process variance or both at the same time, without giving much importance to shift in the shape. To this end, it is worthy to compare some traditional monitoring procedures, such as, the $\overline{X}$ chart for solely monitoring the process mean, the S chart for monitoring the process variance, as well as the charts based on ordinary max or distance statistic for jointly monitoring both the mean and variance, with the NSN-LR and NSN-DS charts. Such a comparative performance study will reflect whether the proposed schemes are really suitable in detecting an overall process shift quickly compared to traditional schemes.

Following are the plotting statistics of the existing schemes for monitoring the process mean, process variance or both, used for the comparative study:

$\overline{X}$ chart:
$$Q_{\overline{X}}\left(\boldsymbol{X_j}\right) = \left|\frac{\overline{X}_j - \mu}{\sigma/\sqrt{n}}\right|;$$

S chart:
$$Q_S\left(\boldsymbol{X_j}\right) = \left|\Phi^{-1}\left\{F_{\chi^2_{(n-1)}}\left(\frac{(n-1)S_j^2}{\sigma^2}\right)\right\}\right|;$$

max chart:
$$Q_M\left(\boldsymbol{X_j}\right) = \max\left\{\left|\frac{\overline{X}_j - \mu}{\sigma/\sqrt{n}}\right|, \left|\Phi^{-1}\left\{F_{\chi^2_{(n-1)}}\left(\frac{(n-1)S_j^2}{\sigma^2}\right)\right\}\right|\right\};$$

distance chart:
$$Q_D\left(\boldsymbol{X_j}\right) = \sqrt{\left(\frac{\overline{X}_j - \mu}{\sigma/\sqrt{n}}\right)^2 + \left(\Phi^{-1}\left\{F_{\chi^2_{(n-1)}}\left(\frac{(n-1)S_j^2}{\sigma^2}\right)\right\}\right)^2}.$$

We compare the above four schemes with the proposed NSN-LR chart and NSN-DS chart under the similar OOC set-up used in Section 4.1. For a fair comparison, we only consider the standard Shewhart-type version of all the charts involved. In Table 3, we present the mean, the standard deviation and the skewness coefficient of the $ASN(\lambda)$ distribution for various values of λ_1, considered in Section 4.1.

Table 3:   Means, standard deviations and skewness coefficients of the ASN distribution under IC value and various OOC values of λ.

IC Situation			
λ_0	μ_0	σ_0	γ_0
0	0	1	0

OOC Situation			
λ_1	μ_1	σ_1	γ_1
0.3	0.2293	0.9734	0.0056
0.5	0.3568	0.9342	0.0239
1	0.5642	0.8256	0.1369
2	0.7136	0.7005	0.4538
3	0.7569	0.6535	0.6670
5	0.7824	0.6228	0.8510
10	0.7939	0.6080	0.9556
$+\infty$	0.7979	0.6028	0.9953

From Table 3, it is easy to see that when λ increases from 0 to $+\infty$, μ and γ increase, but σ decreases. One may check that when λ_1 decreases from 0 to $-\infty$, all three measures, the mean, the variance and the skewness coefficient decrease. To be precise, in our simulation set-up, if there is a shift from $\lambda = 0$ to $\lambda_1(-\lambda_1)$, the mean $\mu = 0$ will change to $\mu_1(-\mu_1)$, the standard deviation $\sigma = 0$ will change to $\sigma_1(\sigma_1)$, and $\gamma = 0$ will change to $\gamma_1(-\gamma_1)$. For brevity, we omit the case of decreasing shift in λ.

In Table 4, we summarize the result of performance comparisons among the NSN-LR chart, the NSN-DS chart and the four traditional alternatives (i.e.,

Table 4: The OOC performance comparisons among the NSN-LR chart, the NSN-DS chart and other alternatives for various λ_1 and n when $IC\text{-}ARL = 370$.

λ_1	$n = 5$					
	NSN-LR chart	NSN-DS chart	$\overline{X}$ chart	S chart	max chart	distance chart
0.3		230.85 (229.96)	**181.20 (180.84)**	421.72 (422.96)	244.14 (243.51)	240.61 (239.75)
0.5		145.69 (145.00)	**106.09 (105.12)**	454.31 (453.81)	160.33 (158.94)	159.68 (159.26)
1		60.77 (60.21)	**52.23 (51.62)**	337.54 (337.87)	83.64 (82.75)	81.57 (80.57)
2	Not Useful	30.19 **(29.60)**	36.06 (35.38)	164.33 (163.60)	55.55 (54.98)	52.02 (51.27)
3		**24.70 (24.12)**	33.17 (32.55)	113.58 (113.55)	48.38 (47.73)	46.10 (45.50)
5		**22.45 (21.87)**	31.74 (31.18)	83.34 (83.27)	43.36 (42.79)	42.89 (42.42)
10		**21.97 (21.41)**	31.12 (30.60)	69.16 (69.13)	40.41 (39.78)	41.24 (40.82)

λ_1	$n = 10$					
	NSN-LR chart	NSN-DS chart	$\overline{X}$ chart	S chart	max chart	distance chart
0.3	129.81 (128.97)	123.92 (122.95)	**102.21 (101.85)**	410.33 (409.76)	150.01 (150.07)	149.23 (147.96)
0.5	55.69 (54.73)	51.78 (51.16)	**43.94 (43.37)**	380.25 (378.66)	68.56 (68.16)	68.96 (67.96)
1	13.06 (12.53)	**12.04 (11.53)**	13.99 (13.45)	159.10 (159.37)	21.24 (20.76)	19.31 (18.78)
2	**3.78 (3.23)**	3.84 (3.31)	6.91 (6.38)	41.70 (41.34)	9.63 (9.10)	6.82 (6.28)
3	**2.31 (1.74)**	2.61 (2.05)	5.71 (5.18)	23.12 (22.59)	7.42 (6.91)	4.69 (4.15)
5	**1.55 (0.93)**	2.01 (1.43)	5.11 (4.58)	15.43 (14.98)	6.18 (5.64)	3.63 (3.09)
10	**1.18 (0.46)**	1.75 (1.15)	4.86 (4.33)	12.65 (12.18)	5.62 (5.08)	3.18 (2.62)

λ_1	$n = 15$					
	NSN-LR chart	NSN-DS chart	$\overline{X}$ chart	S chart	max chart	distance chart
0.3	73.57 (73.20)	74.68 (74.47)	**66.56 (66.18)**	397.62 (396.70)	101.11 (100.47)	101.42 (100.85)
0.5	24.61 (24.10)	24.98 (24.46)	**23.82 (23.17)**	320.89 (321.72)	36.77 (36.22)	37.22 (36.61)
1	**4.56 (4.02)**	4.80 (4.25)	6.19 (5.67)	90.72 (89.86)	8.74 (8.27)	7.58 (7.06)
2	**1.46 (0.82)**	1.62 (1.00)	2.77 (2.21)	17.09 (16.60)	3.43 (2.88)	2.28 (1.69)
3	**1.11 (0.35)**	1.23 (0.53)	2.24 (1.66)	9.09 (8.55)	2.55 (1.98)	1.57 (0.95)
5	**1.01 (0.11)**	1.07 (0.28)	1.99 (1.40)	6.12 (5.58)	2.11 (1.52)	1.28 (0.59)
10	**1.00 (0.01)**	1.02 (0.16)	1.88 (1.29)	5.10 (4.56)	1.92 (1.32)	1.17 (0.45)

λ_1	$n = 25$					
	NSN-LR chart	NSN-DS chart	$\overline{X}$ chart	S chart	max chart	distance chart
0.3	35.52 (34.95)	36.60 (36.09)	**34.95 (34.50)**	373.78 (375.17)	53.70 (53.19)	54.59 (53.98)
0.5	**9.49 (9.00)**	9.99 (9.50)	10.34 (9.88)	237.89 (238.12)	15.01 (14.54)	15.22 (14.70)
1	**1.80 (1.21)**	1.93 (1.34)	2.41 (1.85)	40.32 (39.85)	3.01 (2.47)	2.58 (2.02)
2	**1.02 (0.16)**	1.05 (0.22)	1.26 (0.58)	5.76 (5.20)	1.33 (0.66)	1.10 (0.33)
3	**1.00 (0.03)**	**1.00 (0.06)**	1.13 (0.38)	3.21 (2.64)	1.12 (0.36)	1.01 (0.11)
5	**1.00 (0.00)**	**1.00 (0.01)**	1.07 (0.28)	2.35 (1.77)	1.04 (0.20)	**1.00 (0.03)**
10	**1.00 (0.00)**	**1.00 (0.00)**	1.05 (0.23)	2.06 (1.46)	1.02 (0.13)	**1.00 (0.01)**

the $\overline{X}$ chart, the S chart, the max chart, and the distance chart) in the cases of $\lambda_1 = 0.3$, 0.5, 1, 2, 3, 5, 10, and $n = 5$, 10, 15, 25. From Table 4, we see that our proposed NSN-LR chart and NSN-DS chart outperform the four traditional charts in most of the cases, except for very small shift in asymmetry parameter. To be precise, when λ_1 is very small, the $\overline{X}$ chart is slightly more effective when sample size n is also small. Further, we observe that, as the test sample size n increases, our proposed NSN-LR and NSN-DS schemes become very competitive to the traditional $\overline{X}$ chart even for small shift in asymmetry parameter. In general, among these traditional alternatives, the $\overline{X}$ chart performs the best when λ_1 is small and then the distance chart supersedes the $\overline{X}$ chart when λ_1 gets larger. The max chart performs similarly as the distance chart. The S chart performs the worst compared to the other schemes, probably due to the decreasing variance. The performance of these traditional charts are, however, better than the other four charts introduced in this paper based on various measures of skewness. We further notice that, when the test sample size is large enough and the shift in the asymmetry parameter is also very large, that is, both the values of n and λ_1 are relatively large, all four traditional schemes considered here display commanding performance similar to the NSN-LR chart or the NSN-DS chart.

In summary, we can conclude that our proposed NSN-LR chart and NSN-DS chart have some distinct advantages in detecting a shift when the process distribution deviates from normal to skew-normal, specially when λ_1 is moderate-to-large. Otherwise, one may simply apply the traditional alternative, like $\overline{X}$ chart for detecting shifts in the process mean. Nevertheless, using $\overline{X}$ chart may be misleading in practice as it is designed for capturing a shift in the mean of a normally distributed process. It may not reflect the actual phenomenon, that is, the shift has taken place in the distribution itself. It may not be realized that the assignable cause has actually led to a disruption of symmetry of the process distribution. The effect of shift in asymmetry parameter would be confounded if we use any of the traditional charts. This clarifies the motivation behind developing the NSN-type control charts.
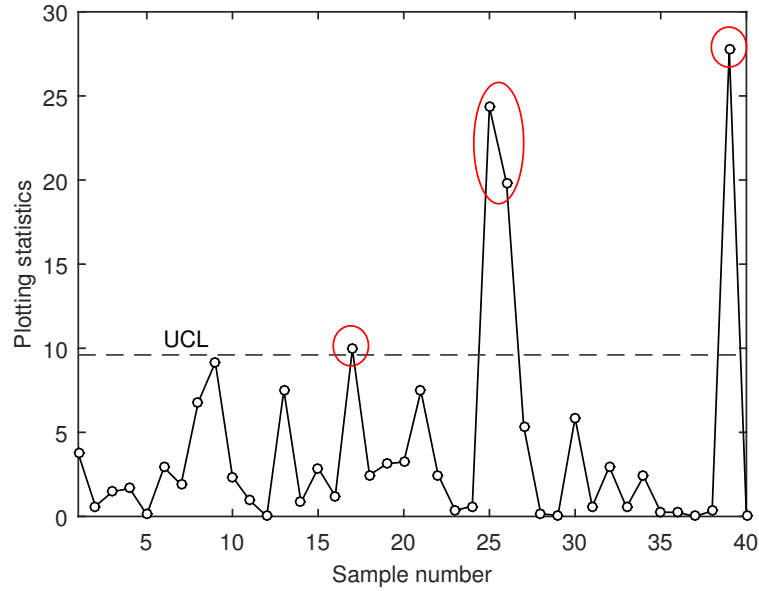
5.   APPLICATION TO A MANUFACTURING PROCESS

In this section, we revisit the real example of a cork stopper's process production presented by Figueiredo and Gomes [9]. Figueiredo and Gomes [9] considered a consecutive sample of size $n = 1000$, related to corks' diameters as well as some other measurements from the production process. They applied the Shapiro test for normality and the Kolmogorov-Smirnov (K-S) test for goodness of fit of the ASN distribution on the 1000 data points. They noted that the Shapiro test rejects the normality of the diameter data at 5% level of significance, but the K-S test accepts the ASN distribution as a decent model for the diameter data.

They concluded accordingly that the ASN distribution may be considered to model the diameter data instead of the normal distribution.
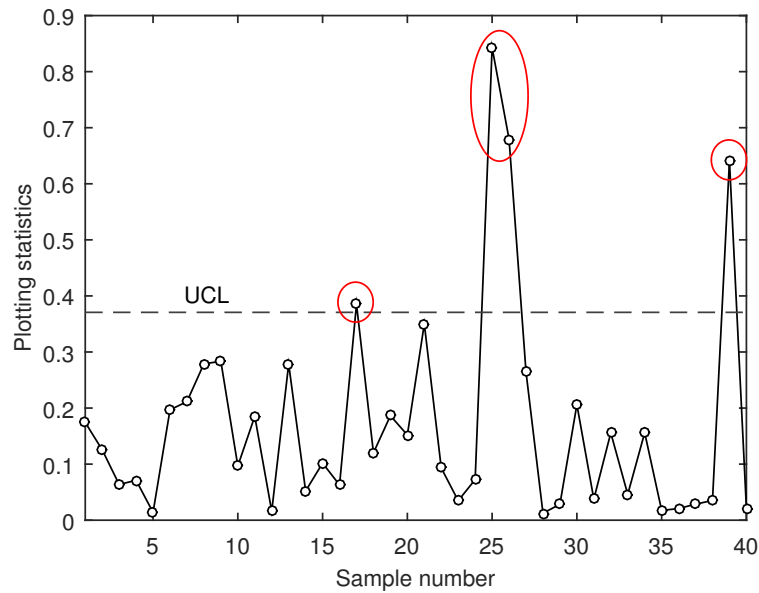
Nevertheless, we revisit the diameter data set, and observe that during the initial stage of production, the underlying data distribution appears to be normal. We note that for the first 200 observations on corks' diameter, the p-value of the Shapiro test is very high and is 0.9296. This finding strongly supports the normality assumption (also see Figure 1) for the initial stage of production. We also notice that the process distribution deviates from normality and gradually becomes skew-normal (the p-value of the Shapiro test for normality gradually becomes lower and soon becomes less than 1%) as the production continues, probably due to unobservable occurrence of one or more assignable cause(s) at some point of time. Hence, we may argue that the process distribution has deviated from the normality and tends to follow an ASN distribution with some non-zero asymmetry parameter.

In this context, we illustrate the implementation of the proposed Shewhart-type NSN-LR and NSN-DS charts for monitoring the diameter data observed from the cork stopper's process production. We take the first 200 observations related to corks' diameter as the IC sample which is also referred to as the Phase I observations in literature. We obtain the estimates for the mean value and the standard deviation as 24.0695 and 0.1459 respectively. We use these estimates to approximate the true process parameters. The following 800 observations may be regarded as the Phase II data that consists of $m = 40$ subgroups each of size $n = 20$. For $n = 20$ and a target *IC-ARL* of 370, we see from Table 1, the control limits for the two charts are, respectively, $H_{LR} = 9.6034$ and $H_{DS} = 0.3707$. Hereafter, we compute the LR and DS statistics for these 40 subgroups and plot them in Figure 3 and 4, along with the respective UCL.

We see that the movement of the plotting statistics in these two charts are very similar in nature. We receive the first signal at the 17th test sample for both charts. Moreover, several points fall above the UCL in both these charts. We may consider this as a strong evidence of deviation of process distribution and therefore, may conclude that the initial assumption of normally distributed process is no longer valid and the process distribution becomes asymmetric. To be precise, the ASN distribution (with some non-zero asymmetry parameter) emerges as the new process distribution. Since in the whole data set, normally distributed IC data have been contaminated (mixed) with the shifted data which are generated from the OOC process, this easily leads to an illusion that the data inherently follows an ASN distribution.

Figure 3:   The NSN-LR chart for the corks' diameter data.

Figure 4:   The NSN-DS chart for the corks' diameter data.

6.   CONCLUDING REMARKS

In this paper, we study on the statistical process monitoring problem in regard to detecting a shift from normal to skew-normal. A class of possible test statistics are thoroughly examined and we find that the proposed monitoring procedures based on the likelihood ratio statistic and the sample distance skewness statistic operate most competitively, especially the latter. Therefore, these two approaches are expected to be very useful in practice to monitor the asymmetry parameter of an ASN distribution and to detect a process shift from normality to skew-normal with $\lambda \neq 0$.

In the present context, we study the performance of the standard Shewhart-type version for all charts. It is well-known that the Shewhart-type charts are usually good for detecting large and abrupt shifts in a process, however, the change in skewness actually is relatively small even if λ_1 gets very large for the ASN distribution. Thus, a straightforward extension of the proposed monitoring schemes under the EWMA or CUSUM set-up may be considered as a future research problem. Further, more researches on the economic and the economic-statistical design of the NSN-LR and NSN-DS charts are highly warranted in future.

In addition, as stated before, further research on simultaneous monitoring of all the parameters (location, scale and shape) of the ASN distribution needs to be studied in detail. It will also be an interesting future research problem to develop process monitoring schemes when the parameters are unknown and estimated from the reference sample. Clearly, the present work may lead to some interesting future research problems.

ACKNOWLEDGMENTS

REFERENCES

[1]   ARELLANO-VALLE, R.B.; GÓMEZ, H.W. and QUINTANA, F.A. (2004). A new class of skew-normal distributions, *Communications in Statistics – Theory and Methods*, **33**, 1465–1480.

[2]   AZZALINI, A. (1985). A class of distributions which includes the normal ones, *Scandinavian Journal of Statistics*, **12**, 171–178.

[3]   AZZALINI, A. (1986). Further results on a class of distributions which includes the normal ones, *Statistica*, **46**, 199–208.

[4]   AZZALINI, A. (2005). The skew-normal distribution and related multivariate families, *Scandinavian Journal of Statistics*, **32**, 159–188.

[5]   BARTOLETTI, S. and LOPERFIDO, N. (2009). Modelling air pollution data by the skew-normal distribution, *Stochastic Environmental Research and Risk Assessment*, **24**, 513–517.

[6]   CASTAGLIOLA, P. (2005). A new S2-EWMA control chart for monitoring the process variance, *Quality and Reliability Engineering International*, **21**, 781–794.

[7]   CHEN, J.T.; GUPTA, A.K. and NGUYEN, T.T. (2004). The density of the skew normal sample mean and its applications, *Journal of Statistical Computation and Simulation*, **74**, 487–494.

[8]   FERREIRA, J.T.A.S. and STEEL, M.F.J. (2006). A constructive representation of univariate skewed distributions, *Journal of the American Statistical Association*, **101**, 823–829.

[9]   FIGUEIREDO, F. and GOMES, M.I. (2013). The skew-normal distribution in SPC, *REVSTAT – Statistical Journal*, **11**, 83–104.

[10]   FIGUEIREDO, F. and GOMES, M.I. (2015). The role of asymmetric families of distributions in eliminating risk, *Theory and Practice of Risk Assessment*, **136**, 267–277.

[11]   FRUHWIRTH-SCHNATTER, S. and PYNE, S. (2010). Bayesian inference for finite mixtures of univariate and multivariate skew-normal and skew-t distributions, *Biostatistics*, **11**, 317–336.

[12]   GENTON, M.G.; HE, L. and LIU, X. (2001). Moments of skew-normal random vectors and their quadratic forms, *Statistics & Probability Letters*, **51**, 319–325.

[13]   GÓMEZ, H.W.; CASTRO, L.M.; SALINAS, H.S. and BOLFARINE, H. (2010). Properties and inference on the skew-curved-symmetric family of distributions, *Communications in Statistics – Theory and Methods*, **39**, 884–898.

[14]   GUO, B. and WANG, B.X. (2015). The design of the ARL-unbiased S2 chart when the in-control variance is estimated, *Quality and Reliability Engineering International*, **31**, 501–511.

[15]   HAWKINS, D.M. and DENG, Q. (2009). Combined charts for mean and variance information, *Journal of Quality Technology*, **41**, 415–425.

[16]   HENZE, N. (1986). A probabilistic representation of the 'skew-normal' distribution, *Scandinavian Journal of Statistics*, **13**, 271–275.

[17] Hosking, J.R.M. (1990). L-moments: Analysis and estimation of distributions using linear combinations of order statistics, *Journal of the Royal Statistical Society: Series B*, **52**, 105–124.

[18] Khoo, M.B.C.; Wong, V.H.; Wu, Z. and Castagliola, P. (2012). Optimal design of the synthetic chart for the process mean based on median run length, *IIE Transactions*, **44**, 765–779.

[19] Knoth, S. (2015). Run length quantiles of EWMA control charts monitoring normal mean or/and variance, *International Journal of Production Research*, **53**, 4629–4647.

[20] Li, C.; Mukherjee, A.; Su, Q. and Xie, M. (2016). Design and implementation of two CUSUM schemes for simultaneously monitoring the process mean and variance with unknown parameters, *Quality and Reliability Engineering International*, **32**, 2961–2975.

[21] Li, C.-I.; Su, N.-C.; Su, P.-F. and Shyr, Y. (2014). The design of X-bar and R control charts for skew normal distributed data, *Communications in Statistics – Theory and Methods*, **43**, 4908–4924.

[22] Li, Z.; Zou, C.; Wang, Z. and Huwang, L. (2013). A multivariate sign chart for monitoring process shape parameters, *Journal of Quality Technology*, **45**, 149–165.

[23] Mameli, V. and Musio, M. (2013). A generalization of the skew-normal distribution: The beta skew-normal, *Communications in Statistics – Theory and Methods*, **42**, 2229–2244.

[24] McCracken, A.K.; Chakraborti, S. and Mukherjee, A. (2013). Control charts for simultaneous monitoring of unknown mean and variance of normally distributed processes, *Journal of Quality Technology*, **45**, 360–376.

[25] Mukherjee, A.; Abd-Elfattah, A.M. and Pukait, B. (2013). A rule of thumb for testing symmetry about an unknown median against a long right tail, *Journal of Statistical Computation and Simulation*, **84**, 2138–2155.

[26] Peng, Y.; Xu, L. and Reynolds, M.R., Jr. (2015). The design of the variable sampling interval generalized likelihood ratio chart for monitoring the process mean, *Quality and Reliability Engineering International*, **31**, 291–296.

[27] Rahman, S. and Hossain, F. (2008). A forensic look at groundwater arsenic contamination in Bangladesh, *Environ Forensics*, **9**, 364–374.

[28] Razzaghi, M. (2014). A hierarchical model for the skew-normal distribution with application in developmental neurotoxicology, *Communications in Statistics – Theory and Methods*, **43**, 1859–1872.

[29] Reynolds, M.R., Jr.; Lou, J.; Lee, J. and Wang, S. (2013). The design of GLR control charts for monitoring the process mean and variance, *Journal of Quality Technology*, **45**, 34–60.

[30] Ross, G.J. and Adams, N.M. (2012). Two nonparametric control charts for detecting arbitrary distribution changes, *Journal of Quality Technology*, **44**, 102–116.

[31] Ryu, J.-H.; Wan, H. and Kim, S. (2010). Optimal design of a CUSUM chart for a mean shift of unknown size, *Journal of Quality Technology*, **42**, 311–326.

[32] Sheu, S.-H.; Huang, C.-J. and Hsu, T.-S. (2012). Extended maximum generally weighted moving average control chart for monitoring process mean and variability, *Computers & Industrial Engineering*, **62**, 216–225.

[33]   SHU, L.; YEUNG, H.-F. and JIANG, W. (2010). An adaptive CUSUM procedure for signaling process variance changes of unknown sizes, *Journal of Quality Technology*, **42**, 69–85.

[34]   SU, N.-C.; CHIANG, J.-Y.; CHEN, S.-C.; TSAI, T.-R. and SHYR, Y. (2014). Economic design of two-stage control charts with skewed and dependent measurements, *The International Journal of Advanced Manufacturing Technology*, **73**, 1387–1397.

[35]   SU, N.-C. and GUPTA, A.K. (2015). On some sampling distributions for skew-normal population, *Journal of Statistical Computation and Simulation*, **85**, 3549–3559.

[36]   TSAI, T.-R. (2007). Skew normal distribution and the design of control charts for averages, *International Journal of Reliability, Quality and Safety Engineering*, **14**, 49–63.

[37]   TSIAMYRTZIS, P. and HAWKINS, D.M. (2005). A Bayesian scheme to detect changes in the mean of a short-run process, *Technometrics*, **47**, 446–456.

[38]   VINCENT, R. and WALSH, T.D. (1997). Quantitative measurement of symmetry in CBED patterns, *Ultramicroscopy*, **70**, 83–94.

[39]   WU, Z.; YANG, M.; KHOO, M.B.C. and YU, F.J. (2010). Optimization designs and performance comparison of two CUSUM schemes for monitoring process shifts in mean and variance, *European Journal of Operational Research*, **205**, 136–150.

[40]   ZHANG, G. (2014). Improved R and s control charts for monitoring the process variance, *Journal of Applied Statistics*, **41**, 1260–1273.

[41]   ZOU, C. and TSUNG, F. (2010). Likelihood ratio-based distribution-free EWMA control charts, *Journal of Quality Technology*, **42**, 174–196.